



# Distributed Obstacles Avoidance For UAVs Formation Using Consensus-based Switching Topology

Kheireddine Choutri<sup>1</sup>, Mohand Lagha<sup>1</sup> and Laurent Dala<sup>2</sup>

<sup>1</sup>Aeronautical Sciences Laboratory Aeronautical and Spatial Studies Institute University Blida1, Algeria

<sup>2</sup>Department of Mechanical and Construction Engineering, Northumbria University, United Kingdom

Received 12 Nov.2018, Revised 2 Feb. 2019, Accepted 25 Feb. 2019, Published 1 Mar. 2019

**Abstract:** Nowadays, most of the recent researches are focusing on the use of multi-UAVs in both civil and military applications. Multiple robots can offer many advantages compared to a single one such as reliability, time decreasing and various simultaneous interventions. However, solving the formation control and obstacles avoidance problems is still a big challenge. This paper proposes a distributed strategy for UAVs formation control and obstacles avoidance using a consensus-based switching topology. This novel approach allows UAVs to keep the desired topology and switch it in the event of avoiding obstacles. A double loop control structure is designed using a backstepping controller for tracking of the reference path, while a Sliding Mode Controller (SMC) is adopted for formation control. Furthermore, collaborative obstacles avoidance is assured by switching the swarm topology. Numerical simulations show the efficiency of the proposed strategy.

**Keywords:** Quadrotors, Multi-UAVs, Obstacles Avoidance, Switching Topology, Formation Control.

## 1. INTRODUCTION

In the last recent years, multi-agents formation control problems have become widely investigated in the research community. Compared with a single UAV, a group of collaborative UAVs can fulfill more difficult tasks and accomplish complex objectives. Different strategies and architectures have been proposed in the literature, such as behavior-based [1], virtual structure [2], potential field [3] and leader-follower [4-7]. In the centralized leader-follower (L-F) scenario, one of the agents designated as “leader” has the reference motion to be tracked by the other agents “followers”. To act cooperatively, the leader spreads its states among the rest of the swarm employing proper communication link; thus any single failure of the leader will lead to failure in the whole mission.

In a formation control, quadrotors are not physically coupled. However, their relative motions are strongly constrained to keep the formation. In order to achieve precise formation control of multiple UAVs such as quadrotors, an accurate position control of each one is required [8-10]. For formation control, consensus algorithms have been extensively studied in the literature [4,7]. Based on consensus theory, it is clear that the achievement of formation depends not only on the

individual UAV dynamics but also the interaction topologies between UAVs which is modeled by the graph theory. In practical applications, topology of UAV swarm systems may be switching due to the fact that the communication channel may fail or a new leader is elected. Formation control for UAVs with directed and switching topologies is studied in [11]. Reference [12] proposes a novel switching method based on the binary-tree network (BTN) to realize the transformations between the V-shape and the complete binary tree shape (CBT-shape) topologies.

Many control mechanisms were used to hold the formation topology, the theory of multiple UAVs formation control can be found in [7]. References [13,14] propose a second-order consensus algorithm to follow a predetermined external reference, while [4,15,16] describes the formation control problem as a position control problem to be solved. While the precedent control techniques were able to maintain the formation, an estimation of the position for the leader as well as the followers is needed. An attitude control technique is used for spacecraft formation vehicles such as in [17-18] where robust attitude coordinated control is used. For quadrotors, reference [19] proposes a transformation control technique to convert the position control to an

attitude control problem. After this, the formation attitude stability is then assured using a backstepping controller.

In order to operate safely and to accomplish mission tasks, one of the essential criteria required for the UAVs is the ability to avoid collisions with other members of swarms and environmental obstacles. A survey of UAVs obstacles avoidance is presented in [20]. Paper [21] proposes two efficient algorithms: conflict detection (CD) algorithm and conflict resolution (CR) algorithm for cooperative multi-UAV collision avoidance system. The work in [22] proposes modified tentacle formation flight and collision avoidance algorithm for multiple UAVs in unstructured environments, while [23] developed an autonomous navigation and avoiding obstacles along the trajectory without any pilot inputs in an outdoor environment. In [24], the author's present directional collision avoidance with obstacles in swarming applications through the implementation of relative position based cascaded PID position and velocity controllers. Furthermore, reference [25] presents a collision avoidance method for multiple UAVs and other non-cooperative aircraft based on velocity planning and taking into account the trajectory prediction under uncertainties. Finally, reference [2] deals with a behavior-based decentralized control strategy for UAV swarming by using artificial potential functions and sliding mode control technique. However the previously cited papers were able to deal with the obstacle avoidance problem within a swarm of UAVs, but no one has optimized the generated trajectory.

This paper introduces a distributed strategy for UAVs formation control and obstacles avoidance using a consensus-based switching topology. The novelty of this approach is that the UAVs can keep the desired topology while tracking the reference path and switch it to avoid obstacles.

Based on a consensus-attitude approach, the formation topology is maintained with a minimum of a sharing data, and the controller is robust to any external disturbances. Furthermore, both of trajectory tracking and formation control algorithms are based on a double loop control structure with backstepping/SMC controller.

This article is organized as follow: Section 2 gives a brief background over graph theory and consensus dynamics. The dynamic model of a quadrotors is described in Section 3. Section 4 introduces a single quadrotors controller design in the first part, while the second part shows the formation control design using SMC controller. Trajectory generation and obstacle avoidance algorithms can be found in Section 5. Section 6 discusses the simulation results with many proposed scenarios. Finally, in Section 7 conclusions as well as future recommendations are given.

## 2. DISTRIBUTED L-F FORMATION

### A. Formation Configuration

The distributed formation control with L-F configuration is depicted in Fig.1. The red quadrotors represent the leaders, while the others are followers. The proposed leader-follower formation has the following novelties comparing to the existing works.

- Distrusted formation control: The quadrotors do not have any global knowledge, thus no single centralized decision maker exists.
- Multiple and changeable leaders: the number of leaders may be higher than one, the statue (leader or follower) of the agent is changeable.
- Interactions between leaders and followers: the leader(s) can be affected by their neighboring followers.

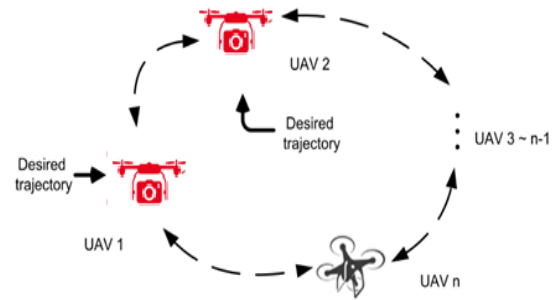


Figure 1. Distributed formation control with L-F configuration

The difficulty of this formation structure is that the followers do not know about the formation trajectory. They only depend on the states of their neighbors (attitude) in order to accomplish the formation task. Therefore, the interactions are important for the followers, not only for the reason of collision avoidance but also for formation.

**Assumption 1.** In the investigated leader-follower formation problem, only the leader is aware of the formation task, and the remaining UAVs interact with each other or with the leaders through a rigid or switching topology.

### B. Consensus Dynamics

Consider  $x_i(t) \in R$  to be the  $i$ -th node's state at time  $t$  on which agreement is required for all nodes. The continuous-time consensus dynamics is defined over the graph  $\mathcal{G} = (\mathcal{V}, \mathcal{E})$  as:

$$\dot{x}_i(t) = \sum_{\{v_i, v_j\} \in \mathcal{E}} (x_j(t) - x_i(t)) \quad (2)$$

Thus, to update the  $i$ -th node's state, only the relative state of node  $i$ 's neighbor's state is required. In a compact form with  $x(t) \in R$ , the collective dynamics is represented as:

$$\dot{x}(t) = -L x(t) \tag{3}$$

With  $L$ , being the graph Laplacian matrix of the underlying interaction topology, described in the previous subsection. For a connected graph  $\mathcal{G}$ , the network dynamics will converge to an agreement on the state, that is  $x_1(t) = x_2(t) = \dots = x_n(t) = \alpha$ , for some constant  $\alpha$ , for all initial conditions. Further, the slowest convergence of the dynamics is determined by  $\lambda_2(L)$  which is a measure of graph connectivity.

**Definition 3.** The L-F consensus of system Eq. 4., is said to be achieved if, for each UAV  $i \in \mathcal{V}$ ,

$$\begin{aligned} \lim_{t \rightarrow \infty} \|x_i - r(t) - d_{i0}\| &= 0 \\ \lim_{t \rightarrow \infty} \|\dot{x}_i - \dot{r}(t)\| &= 0 \quad \text{where } i = 1, \dots, n \end{aligned} \tag{4}$$

for some initial conditions  $x_i(0), i = 1, \dots, n$ . Therefore, the desired position of UAV  $i \in \mathcal{V}$  evolves according to  $x_i^d(t) - r(t) = d_{i0}$  and  $\dot{x}_i^d(t) - \dot{r}(t) = 0$ , then, we obtain:

$$x_i^d(t) = d_{i0} + r(t) \text{ and } \dot{x}_i^d(t) = \dot{r}(t) \tag{5}$$

Let us make a sum of the relative position state vectors. Note that we drop the explicit expression of time in the expressions for the sake of simplicity.

$$\begin{aligned} \sum_{j \in \mathcal{N}_i} (x_i - x_j - d_{ij}) & \quad \text{if } i \text{ is a follower} \\ \sum_{j \in \mathcal{N}_i} (x_i - x_j - d_{ij}) + x_i - r - d_{i0} & \quad \text{if } i \text{ is a leader} \end{aligned} \tag{6}$$

The inter-distance is given by  $d_{ij} = d_{i0} - d_{j0}$ . Then, equations Eq. 6. can be rewritten as follows:

$$\begin{aligned} \sum_{j \in \mathcal{N}_i} ((x_i - r - d_{i0}) - (x_j - r - d_{j0})) & \quad \text{if } i \text{ is a follower} \\ \sum_{j \in \mathcal{N}_i} ((x_i - r - d_{i0}) - (x_j - r - d_{j0})) + x_i - r - d_{i0} & \quad \text{if } i \text{ is a leader} \end{aligned} \tag{7}$$

Let introduce the available desired trajectory for each UAV as follows:

$$\bar{x}_i^d = \frac{1}{|\mathcal{N}_i|} \sum_{j \in \mathcal{N}_i} (x_j + d_{ij}) \quad \text{if } i \text{ is a follower}$$

$$\bar{x}_i^d = \frac{1}{|\mathcal{N}_i + 1|} \left( \sum_{j \in \mathcal{N}_i} (x_j + d_{ij}) + r + d_{i0} \right) \text{ if } i \text{ is a leader} \tag{8}$$

It can be observed that  $\bar{x}_i^d$  is available for UAV  $i$ . Eq. 8. is rewritten in matrix form for all the quadrotors as follows:

$$\begin{bmatrix} x_1 - \bar{x}_1^d \\ \vdots \\ x_n - \bar{x}_n^d \end{bmatrix} = (\tilde{\mathcal{G}} \otimes I_2) \begin{bmatrix} x_1 - x_1^d \\ \vdots \\ x_n - x_n^d \end{bmatrix} \tag{9}$$

Where  $\tilde{\mathcal{G}}$ , represents the normalized interaction matrix. We know that  $\tilde{\mathcal{G}}$  is invertible if the graph of the multi-UAV system is connected with at least one leader. Therefore, if each UAV can precisely track the desired trajectory  $\bar{x}_i^d(t)$ , the formation task is achieved. Its time derivative  $\dot{\bar{x}}_i^d$  can be obtained, which are in terms of the attitude of the neighbors. Note that  $d_{ij}$  is constant in a rigid formation task. In the literature, for instance, where a leaderless multi-agent system is considered, the proposed consensus algorithm leads to a normalized Laplacian matrix. In this paper, since an L-F configuration is considered, a normalized interaction matrix is defined by:

$$\tilde{\mathcal{G}} = (\mathcal{G}^D + \mathcal{G}^L)^{-1} \cdot \mathcal{G} \tag{10}$$

### 3. QUADROTORS DYNAMICS

Let  $E_b\{x_b, y_b, z_b\}$  denotes the body frame attached to the quadrotors while  $E_i\{x_i, y_i, z_i\}$  denotes the inertial frame fixed with the earth while as illustrated in Fig.2.

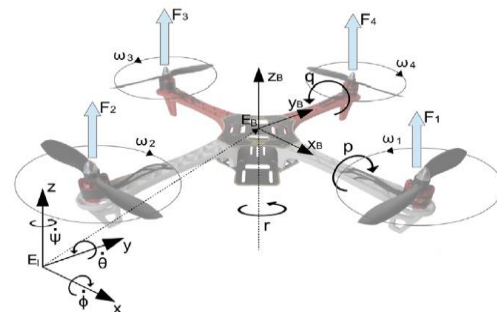


Figure 2. Inertial and body-fixed frame of the quadrotors

For modeling the physics of the quadrotor the Euler-Newton equations for translational and rotational dynamics of a rigid body are used. The dynamical model representing the quadrotor rotations can be given in the state-space form  $\dot{x} = f(x) + g(x,u)$  with  $x = [\varphi \ \theta \ \psi \ \dot{\varphi} \ \dot{\theta} \ \dot{\psi} \ \ddot{\varphi} \ \ddot{\theta} \ \ddot{\psi}]^T$ , is the state vector of the system such as:

$$f = \begin{cases} \dot{x}_1 = x_2 \\ \dot{x}_2 = a_1 x_4 x_6 + a_2 x_4 \Omega + b_1 u_2 \\ \dot{x}_3 = x_4 \\ \dot{x}_4 = a_3 x_2 x_6 + a_4 x_2 \Omega + b_2 u_3 \\ \dot{x}_5 = x_6 \\ \dot{x}_6 = a_5 x_2 x_4 + b_3 u_4 \\ \dot{x}_7 = x_8 \\ \dot{x}_8 = \frac{u_1}{m} u_x \\ \dot{x}_9 = x_{10} \\ \dot{x}_{10} = \frac{u_2}{m} u_y \\ \dot{x}_{11} = x_{12} \\ \dot{x}_{12} = \frac{1}{m} (C_{x_1} S_{x_3} u_1) - g \end{cases} \quad (11)$$

With:

$$\begin{cases} a_1 = \left( \frac{J_y - J_z}{J_x} \right), a_2 = \left( \frac{J_r}{J_x} \right) \\ a_3 = \left( \frac{J_z - J_x}{J_y} \right), a_4 = \left( -\frac{J_r}{J_y} \right) \\ a_5 = \left( \frac{J_x - J_y}{J_z} \right) \\ b_1 = \left( \frac{l}{J_x} \right), b_2 = \left( \frac{l}{J_y} \right), b_3 = \left( \frac{l}{J_z} \right) \end{cases} \begin{cases} U_x = (C_{x_1} S_{x_3} C_{x_5} + S_{x_1} S_{x_5}) \\ U_x = (C_{x_1} S_{x_3} C_{x_5} - S_{x_1} S_{x_5}) \end{cases}$$

With  $J = \text{diag}(J_x, J_y, J_z)$  introduces the inertia matrix with respect to the body-fixed frame,  $J_r$  is the moment of inertia of the rotor,  $m$  and  $g$  represent the vehicle's mass and gravity vector respectively. Equ.12 gives the designed control inputs:

$$\begin{bmatrix} u_1 \\ u_2 \\ u_3 \\ u_4 \end{bmatrix} = \begin{bmatrix} k_T(\omega_1^2 + \omega_2^2 + \omega_3^2 + \omega_4^2) \\ k_T(\omega_1^2 - \omega_2^2 - \omega_3^2 + \omega_4^2) \\ k_T(\omega_1^2 + \omega_2^2 - \omega_3^2 - \omega_4^2) \\ k_D(-\omega_1^2 + \omega_2^2 - \omega_3^2 + \omega_4^2) \end{bmatrix} \quad (12)$$

Quadrotors are a differential system with 4 at outputs [8]. These at outputs are the inertial position of the vehicle,  $x$ ,  $y$ , and  $z$ , and the yaw angle  $\psi$ . By manipulation of the equation of motion, the state vector and input vector can be expressed as a function of the output vector.

$$\begin{aligned} \theta_d &= \arctan\left(\frac{x_8}{x_{12} + g}\right) \\ \varphi_d &= \arctan\left(\frac{x_8}{x_{12} + g} \cdot \cos(\theta_d)\right) \end{aligned} \quad (13)$$

## 4. CONTROLLER DESIGN

### A. Formation Controller

The formation control strategy is as follows: first, the swarm leaders have to track the predefined path, and the followers follow the leader while maintaining the separation distance from the leader. For the position controller, the leader tracks the predefined  $x$ ,  $y$  position trajectory using the reference roll and pitch angles. The leader is then tracking the predefined path with the previously calculated reference attitude angles through the attitude tracking control. On the other hand, the followers have the same control scheme as the leader. Instead of the predefined trajectory given to the leader, the follower's attitude and the separation distance  $d_i$  between the followers and leader are used for the formation control of the followers. Fig.3. illustrates the overall proposed formation control system block diagram. The same backstepping-based control strategy is used for both the leader and the followers.

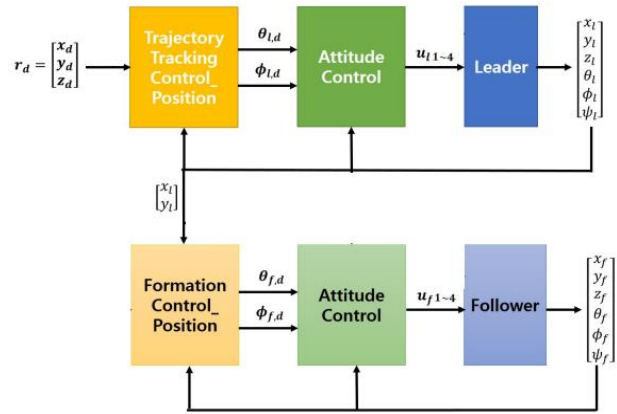


Figure 3. Formation Control Strategy

**Theorem1.** Consider the  $x$ ,  $y$ ,  $z$  position and the  $\varphi$ ,  $\theta$ ,  $\psi$  of the leader/follower in Equ.11. controlled by the actual control inputs in Equ.23. and Equ.24. Then, there exist the design parameters  $k_i > 0$   $i \in \{1, \dots, 12\}$  such that the actual position and attitude control input of the leader/follower in Equ.23. and Equ.24. asymptotically stabilizes the formation error systems in Equ.14.

**Proof.** Let consider the tracking error:

$$e_i = \begin{cases} x_{i,d} - x_i & i \in \{1,3,5,7,9,11\} \\ \dot{x}_{(i-1),d} - \dot{x}_i + k_{(i-1)} e_{(i-1)} & i \in \{2,4,6,8,10,12\} \end{cases} \quad (14)$$

Using the Lyapunov functions as:

$$V_i(x) = \begin{cases} \frac{1}{2} e_i^2 & i \in \{1,3,5,7,9,11\} \\ V_{(i-1)} + \frac{1}{2} e_i^2 & i \in \{2,4,6,8,10,12\} \end{cases} \quad (15)$$

By applying the following algorithm:

For  $i = 1$

$$\begin{cases} e_1 = x_{1d} - x_1 \\ V_1 = \frac{1}{2} e_1^2 \end{cases} \quad (16)$$

And

$$\dot{V}_1 = e_1 \dot{e}_1 = e_1(\dot{x}_{1d} - \dot{x}_2) \quad (17)$$

Using the Lyapunov function, the stability of  $e_1$  can be obtained by introducing a virtual control input  $x_{2d}$  such that:

$$x_{2d} = \dot{x}_{1d} + k_1 e_1 \quad (18)$$

With  $k_1 > 0$  the Equ.18 is then:  $\dot{V}_1 = -k_1 e_1^2$ . Let consider a variable change by making:

$$e_2 = x_2 - \dot{x}_{1d} - k_1 e_1^2 \quad (19)$$

For  $i = 2$

$$\begin{cases} e_2 = x_2 - \dot{x}_{1d} - k_1 e_1^2 \\ V_2 = \frac{1}{2} e_1^2 + \frac{1}{2} e_2^2 \end{cases} \quad (20)$$

And:

$$\dot{V}_2 = e_1 \dot{e}_1 + e_2 \dot{e}_2 \quad (21)$$

Finally:

$$\dot{e}_2 = a_1 x_4 x_6 + a_2 x_4 \Omega + b_1 U_2 - \ddot{x}_{1d} - k_1 \dot{e}_1 \quad (22)$$

The control signal  $U_2$  is obtained such that  $\dot{V}_2 = e_1 \dot{e}_1 + e_2 \dot{e}_2 \leq 0$  as follow:

$$U_2 = \frac{1}{b_1} (-a_1 x_4 x_6 - a_2 x_4 \Omega + \ddot{\phi}_d + k_1 (-k_1 e_1 + e_2) + k_2 e_2 + e_1) \quad (23)$$

The same steps are followed to extract the control signals as follow:

$$\begin{cases} U_3 = \frac{1}{b_2} (-a_3 x_2 x_6 - a_4 x_2 \Omega + \ddot{\theta}_d + k_3 (-k_3 e_3 + e_4) + k_4 e_4 + e_3) \\ U_4 = \frac{1}{b_3} (-a_5 x_2 x_4 + \ddot{\psi}_d + k_5 (-k_5 e_5 + e_6) + k_6 e_6 + e_5) \\ U_x = \frac{m}{U_1} (\ddot{x}_d + k_7 (-k_7 e_7 + e_8) + k_8 e_8 + e_7) \\ U_y = \frac{m}{U_2} (\ddot{y}_d + k_9 (-k_9 e_9 + e_{10}) + k_{10} e_{10} + e_9) \\ U_1 = \frac{m}{C_{x_1} C_{x_3}} (g + \ddot{z}_d + k_{11} (-k_{11} e_{11} + e_{12}) + k_{12} e_{12} + e_{11}) \end{cases} \quad (24)$$

With:  $U_1 \neq 0$  and  $k_i > 0 \quad i \in \{2, \dots, 12\}$

### B. Controller Design

The designed formation controller aims to achieve the desired configuration in X-Y plane for the leader-follower formation. First, the Z altitude is achieved for the swarm into either same or different height. This formation topology is maintained via keeping a constant separation distance  $d$  and an angle  $\alpha$  between each follower and the leader:

$$\begin{aligned} d_x &= -(X_L - X_F) \cos(\psi_L) - (Y_L - Y_F) \sin(\psi_L) \\ d_y &= (X_L - X_F) \sin(\psi_L) - (Y_L - Y_F) \cos(\psi_L) \end{aligned} \quad (25)$$

With  $d_x$  and  $d_y$  are the X and Y coordinates of the actual distance  $d$  as shown in Fig.4.

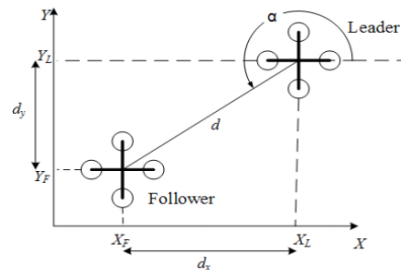


Figure 4. Leader-Followers Formation architecture

**Theorem2.** The formation control can be achieved using the attitude tracking of the leader and the followers. Then, there exist the design parameters  $\lambda_\theta$  and  $\lambda_\varphi$  such that the actual  $\theta, \varphi$  attitude control input of the  $i$ -th follower in Equ.23. and Equ.24. asymptotically stabilizes the formation error systems related to the  $x, y$  position of the  $i$ -th follower in Equ.30.

**Proof.** A first-order sliding mode controller is used to minimize this error. First, a time-varying surface  $s(t)$  is defined by the scalar equation  $s(e, t) = 0$ , where:

$$s(e, t) = \left( \frac{d}{dt} + \lambda \right)^{n-1} e \quad (26)$$

The second-order tracking problem is then transferred to a first-order stabilization problem, thus:

$$\begin{aligned} \dot{s} &= \ddot{e} + \lambda \dot{e} \\ \frac{1}{2} \frac{d}{dt} s^2 &\leq -\eta |s| \end{aligned} \quad (27)$$

Equ.27. is a Lyapunov candidate function chosen for the control law  $u$  to maintain scalar  $s = 0$ . This function states that  $s^2$  is the squared distance to the sliding surface, where  $\eta$  is a positive constant.

As shown in Fig.5.the designed control algorithm is based onSMC controller to keep the formation topology in a perturbed and uncertain environment. The  $x$  and  $y$  formation control errors have to satisfy the following conditions:

$$\begin{aligned} \lim_{t \rightarrow \infty} \|e_x\| &= \|d_x^d - d_x\| = 0 \\ \lim_{t \rightarrow \infty} \|e_y\| &= \|d_y^d - d_y\| = 0 \end{aligned} \quad (28)$$

Where  $d_x^d$  and  $d_y^d$  are the desired distance between the leader and follower in both  $x$  and  $y$  directions respectively.

By assuming a zero yaw angle, the formation can be then controlled according to Equ.25. and Equ.27. for each follower using the following equations:

$$\begin{aligned} \ddot{X}_{F_i} &= \ddot{X}_L + \lambda_x (\dot{X}_L - \dot{X}_{F_i}) \\ \ddot{Y}_{F_i} &= \ddot{Y}_L + \lambda_y (\dot{Y}_L - \dot{Y}_{F_i}) \end{aligned} \quad (29)$$

Finally, by combining Equ.13. and Equ.29. the position control problem is transformed to an attitude control. A direct estimation of the attitude can only be used to control the formation:

$$\begin{aligned} \theta_{F_i} &= \theta_L + \lambda_\theta (\dot{\theta}_L - \dot{\theta}_{F_i}) \\ \varphi_{F_i} &= \varphi_L + \lambda_\varphi (\dot{\varphi}_L - \dot{\varphi}_{F_i}) \end{aligned} \quad (30)$$

where  $\lambda_\theta$  and  $\lambda_\varphi$  are the attitude formation control gains, with  $\lambda_\theta > 0$  and  $\lambda_\varphi > 0$ . Therefore by the Lyapunov stability theorem, the formation error related to the  $i$ -th follower are asymptotically stable.

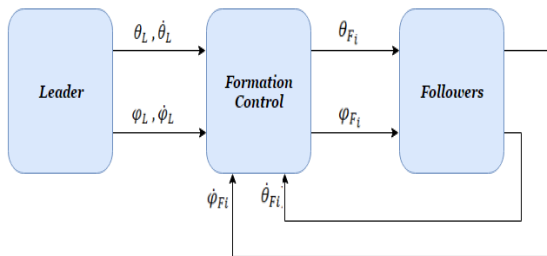


Figure 5. Leader-Followers Formation control

## 5. TRAJECTORY GENERATION & OBSTACLES AVOIDANCE

Algorithm.1 starts with initial positions of all the swarm UAVs, and the only the final position of the leader, the agent's final position is then estimated depending on the formation topology. The mission objective is that the leader reaches its final destination, which means that the distance between the starting and final position converge to zero. The inter-distance between the swarm agents is also supposed to be respected whatever the formation topology is. The optimal path between the starting the final position is a straight line, if exists then the leader and the followers will track it. If any obstacles detected then the function *SelectOptimalPath* will generates the nodes to avoid the obstacles for the leader, which then produces the follower's path. The switching topology formation is called whenever no optimal path can be generated for the followers. The swarm then switches its topology, avoids the obstacles, and comes back to its initial topology if no furthered obstacles are detected.

Algorithm 1. Obstacles Avoidance Algorithm

```

1 Initialization
2 Path( $P_i(i), P_f(i)$ ) all  $i \in \mathcal{V}$ 
3  $P_i \leftarrow P$ 
4 while  $Dist(P_f; P_i) > d_{admissible}$  do
5    $P \leftarrow DrawLine(x_g, x_i)$ 
6   If  $P$  exist
7      $x_i \leftarrow SelectOptimalPath(P_i, P)$ 
8      $P \leftarrow AddPath(P, x_i)$ 
9   If else Obstacle_detected
10     $x_i \leftarrow SelectOptimalPath(P_i, P)$ 
11    switch Line formation
12     $x_i \leftarrow SelectOptimalPath(P_i, P)$ 
13     $P \leftarrow AddPath(P, x_i)$ 
14  end if
15   $i \leftarrow i + 1$ 
16  end while
17 end

```

## 6. SIMULATION RESULTS

This section presents the simulation results related to the quadrotors formation control and obstacles avoidance discussed in the other sections is shown. Many scenarios have carried out depending on the formation control and the different constraints that can occur during a mission.

Table.1 presents all the parameters used in the simulation and adopted to the quadrotors model.

TABLE I. QUADROTORS PARAMETERS

Parameter	Value	Unit
$I_x$	0.00065	$kg.m^2$
$I_y$	0.00065	$kg.m^2$
$I_z$	0.0014	$kg.m^2$
$l$	0.125	$m$
$k_T$	0.001	$kg.m$
$k_D$	0.00002	$kg.m^2$
$m$	0.26	$Kg$

For all the next scenarios 4 quadrotors UAVs are used (Fig .6), the communication link between all the UAVs is supposed to be assured. The aim is that all the UAVs can maintain or switch their formation depending on the faced situation.

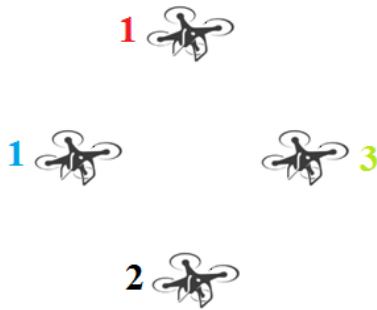


Figure 6. Leader-Followers formation topology

An overview of the simulated cases is described below:

- 1- Scenario1: All the 4 UAVs start from different points and track the desired path while keeping a diamond formation of one leader and three followers.
- 2- Scenario2: In this scenario, the UAVs are tracking the same path as in Scenario 1. An external wind disturbance is presented over the leader and followers.
- 3- Scenario 3: The last scenario simulates the case of the presence of external obstacles. The swarm continues its path to the desired position, and avoids collisions with obstacles or between agents.

A. Scenario 1 : Centralized L-F Formation

As mentioned before, in this scenario four “4” quadrotors UAVs (1 leader and 3 followers) are used in a diamond formation.

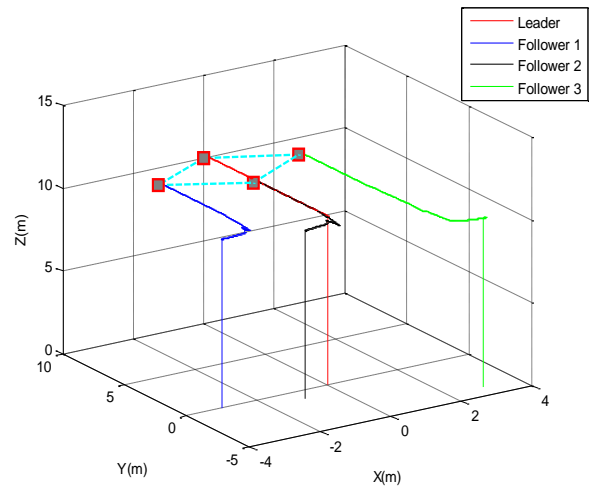


Figure 7. Diamond L-F Formation

The leader begins its route from an initial position  $P_i(x_0, y_0, z_0) = [0; 0; 0]^T$  by reaching the required height  $z$  first, then track the required path in X-Y plane. The leader’s mission is to travel to the point  $P_f(x_0, y_0, z_0) = [0; 10; 10]^T$ . The initial positions of the three followers are at  $F_1(0) = [-3; 0; 0]^T$ ,  $F_2(0) = [-1; -1; 0]^T$  and  $F_3(0) = [3; -4; 0]^T$  respectively, and their desired formation distances with respect to the leader are  $d^{d_{F_1}} = [-2; -2; 0]^T$ ,  $d^{d_{F_2}} = [0; -4; 0]^T$  and  $d^{d_{F_3}} = [2; -2; 0]^T$ .

The aim of this first scenario is to test the controller’s ability to hold the swarm formation while tracking the desired path.

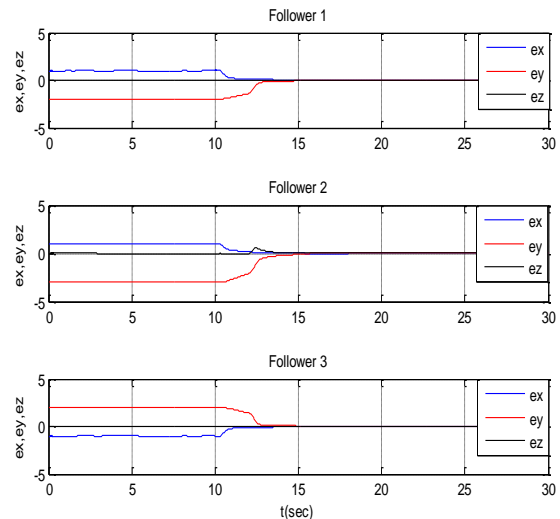


Figure 8. Diamond L-F Formation Tracking Errors

Fig.7. and Fig.8. show that the required formation is achieved with high accuracy. The errors in all coordinates  $x$ ,  $y$  and  $z$  were converged to zero in only 13 sec.

**B. Scenario 2: Centralized L-F Formation with Disturbance:**

In this scenario, the same path is tracked by the UAVs swarm. An external wind gust disturbance is added from the 20 to 25 sec over the  $x, y$  and  $z$ -axes.

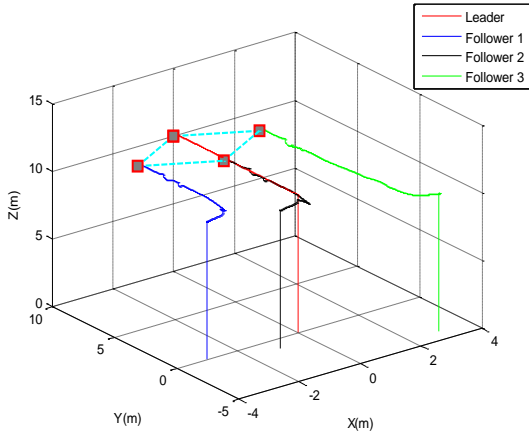


Figure 9. Diamond Formation with Disturbance

The wind gust velocity over the three coordinates is illustrated in Fig.10. The wind speed is between -1 and 1m/s. This kind of scenarios is proposed to test the controller’s robustness and effectiveness.

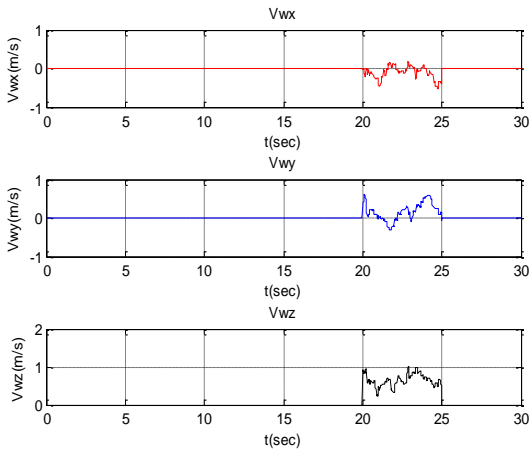


Figure 10. Wind Velocity Profil

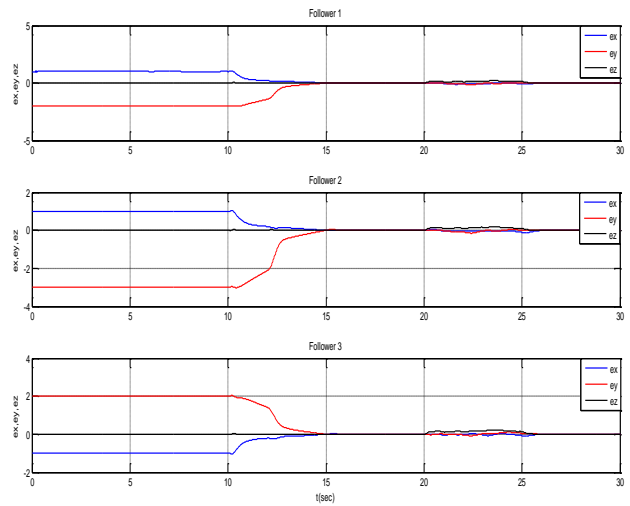


Figure 11. Diamond Formation with Disturbance Tracking Errors

From Fig.9.and Fig.11. it is clear that all the quadrotors were able to maintain their stability, as well as the desired formation during the wind gust disturbance. The formation errors converged to zero after just 1 sec from the end of the disturbance. The swarm agents continue then their desired path while maintaining the same altitude.

**C. Scenario3: Obstacles Avoidance**

For this section, the quadrotors swarm is facing many types of obstacles. The mission is to reach the desired position and avoid the collision with obstacles from a part and the collision between the agents from the other part. For all the simulated cases we consider only the 2D obstacles in the X-Y horizontal plane. The altitude is maintained constant during the entire mission.

**C.1 Case 1:**

In this case the UAVs swarm start from the following positions:  $F_1(0) = [50; 65]^T$ ,  $F_2(0) = [60; 75]^T$ ,  $F_3(0) = [50; 85]^T$  and  $F_4(0) = [40; 75]^T$ . The mission of the leader is to achieve the desired point  $P_f(x_0, y_0) = [50; 15]^T$  and avoid the circular obstacle ( $R = 10$  m) located at  $O_1(x_0, y_0) = [50; 50]^T$ . The separation is 10 m between the agents. The swarm is supposed to hold the diamond formation.



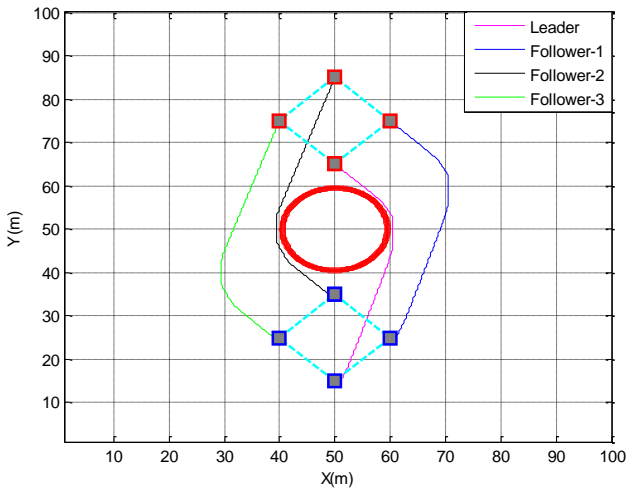


Figure 12. Case -1- Obstacles Avoidance Scenario

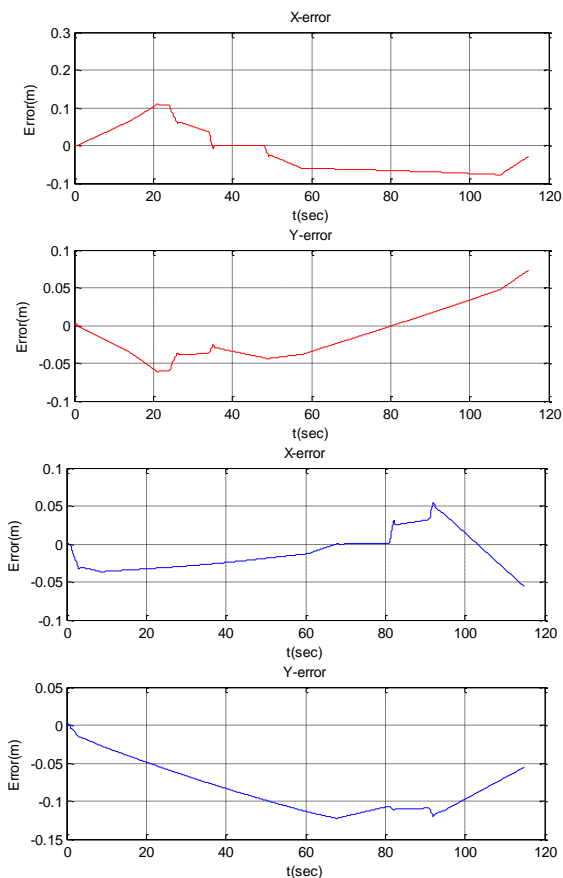


Figure 13. Case -1- Obstacle Avoidance Tracking Errors

From Fig 12. it can be noticed that the swarm was able to avoid the circular obstacle using a distributed formation in order to optimize the energy consumption. The swarm was divided into two teams with two Leaders, one formed by the initial leader and follower 1 and the second created by follower 2 (new leader) and follower 3.

Fig .13. presents the formation error of team 1 and team 2 respectively, it can be noticed that the separation distance (10 m) between the two UAVs was respected with high accuracy in both x and y directions. This reflects the high performance of the formation controller.

C.2 Case 2:

In this case the UAVs swarm start from the following positions:  $F_1(0) = [50; 75]^T$ ,  $F_2(0) = [60; 85]^T$ ,  $F_3(0) = [50; 95]^T$  and  $F_4(0) = [40; 85]^T$ . The mission of the leader is to achieve the desired point  $P_f(x_0, y_0) = [50; 30]^T$  and avoid two circular obstacles ( $R = 10$  m) located at  $O_1(x_1, y_1) = [60; 63]^T$  and  $O_2(x_2, y_2) = [60; 37]^T$ . The separation is 10 m between the agents. The swarm is supposed to hold the diamond formation.

In such case that the swarm cannot pass between the obstacles since the distance between the obstacles is only 6m. The optimal solution for this problem is to switch the formation topology from diamond to linear, then comes back to the initial topology if no further obstacles are detected. Fig.14. shows the case study scenario while the tracking errors are illustrated in Fig.15.

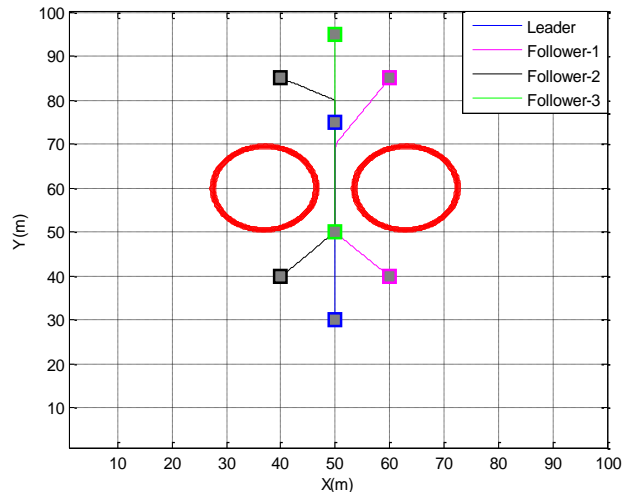


Figure 14. Case -2- Obstacles Avoidance Scenario

From Fig.15.it is clear that the inter-distance between the Leader- Follower 1 , Follower 1- Follower 2 and Follower 2- Follower 3 was respected with high accuracy. The position switching was made in just 5 seconds from the diamond to the line formation and in about 10 seconds to come back to the diamond formation.

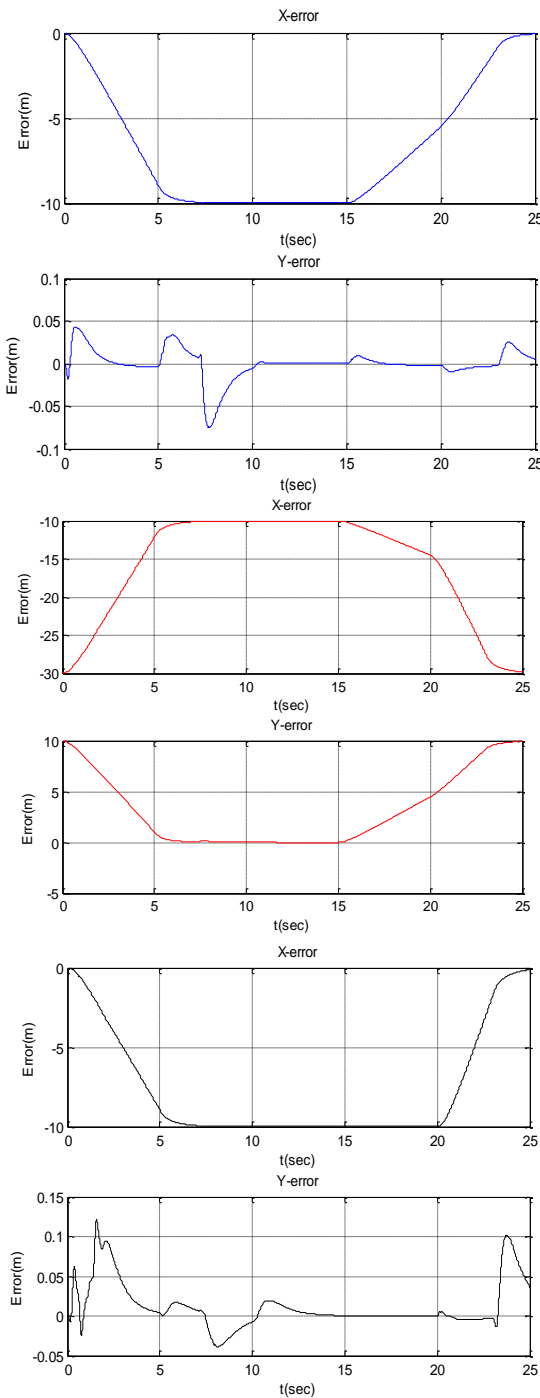


Figure 15. Case -2- Obstacles Avoidance Tracking Errors

C.3 Case 3:

This case is an extension of the second case where a new line obstacle is added, and the swarm is supposed to maintain its linear formation and avoid the new obstacle which is situated at  $O_3(x_3, y_3) = [40: 60; 35]^T$ . The obtained results are shown in Fig. 16.

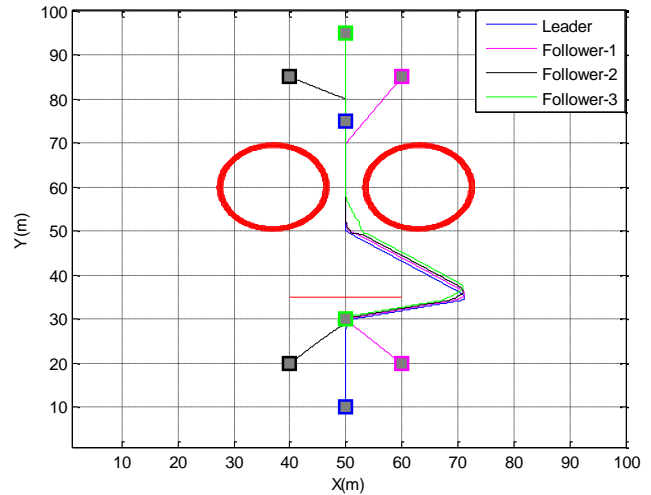


Figure 16. Case -3- Obstacles Avoidance Scenario

As illustrated in Fig.16. the swarm avoids the two circular obstacles as case 2, but this time the leader detect the presence of the new line obstacle, so the swarm maintains its linear formation until the point  $(x, y) = [50; 30]^T$  where the swarm starts it switching back to the diamond formation.

From Fig.17, it is clear that the swarm was able to switch to the linear formation while maintaining the inter-distance between the UAVs. The new line obstacles is are detected and avoided, and the switching to the diamond formation is executed with high accuracy.

7. CONCLUSION

In this paper, we studied the formation control and obstacles avoidance problems of multi-UAVs swarm. A new distributed strategy using a consensus-based switching topology was proposed. The novelty of this approach was that the UAVs were able to keep the desired topology while tracking the reference path and switched it to avoid obstacles.

For the formation control, a consensus-based attitude control was used. The formation was then maintained with only the attitudes data, and the designed controller was robust to external disturbances. Moreover, the agents were able to adapt to varying graph topology due to external obstacles.

The combination of a double loop control structure based on backstepping/SMC controllers was applied to track the reference trajectory, maintain the formation strategy and avoid collisions. Many scenarios were proposed, and all the obtained results were judged to be satisfactory.

For future works, we aim to implement the designed strategy and test it in real scenarios. Many applications and more complicated scenarios could also be considered.

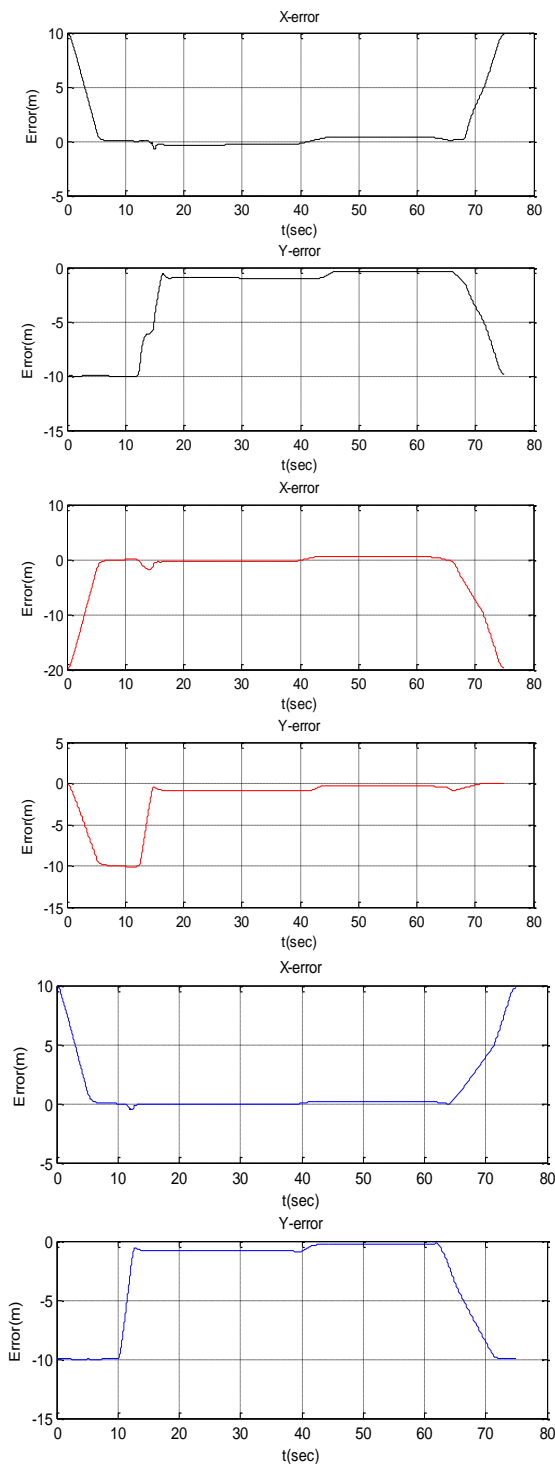


Figure 17. Case -3- Obstacle Avoidance Tracking Errors

**REFERENCES**

[1] Sharma, R. K., & Ghose, D. (2009). Collision avoidance between UAV clusters using swarm intelligence techniques. *International Journal of Systems Science*, 40(5), 521-538.

[2] Dang, A. D., La, H. M., Nguyen, T., & Horn, J. (2017). Distributed formation control for autonomous robots in dynamic environments. *arXiv preprint arXiv:1705.02017*.

[3] Henrique Ribeiro Delgado da Silva.(2012). Formation Control for Unmanned Aerial Vehicles. *ISR & Instituto Superior Tecnico, Technical University of Lisbon, Portugal*.

[4] Ghamry, K. A., & Zhang, Y. (2015, June). Formation control of multiple quadrotors based on leader-follower method. In *Unmanned Aircraft Systems (ICUAS), 2015 International Conference on* (pp. 1037-1042). IEEE.

[5] CHOUTRI, K., LAGHA, M., DALA, L., & LIPATOV, M. (2018, October). Quadrotors UAVs Swarming Control Under Leader-Followers Formation. In *2018 22nd International Conference on System Theory, Control and Computing (ICSTCC)* (pp. 794-799). IEEE.

[6] Hou, Z., & Fantoni, I. (2015, November). Leader-follower formation saturated control for multiple quadrotors with switching topology. In *IEEE Workshop on Research, Education and Development of Unmanned Aerial Systems (RED UAS 2015)* (pp. 8-14).

[7] Hou, Z. (2016). Modeling and formation controller design for multi-quadrotor systems with leader-follower configuration (Doctoral dissertation, Compiègne).

[8] Choutri, K., Lagha, M., Dala, L., & Lipatov, M. (2017, April). Quadrotors trajectory tracking using a differential flatness-quaternion based approach. In *Modeling, Simulation, and Applied Optimization (ICMSAO), 2017 7th International Conference on* (pp. 1-5). IEEE.

[9] Chovancová, A., Fico, T., Hubinský, P., & Duchoň, F. (2016). Comparison of various quaternion-based control methods applied to quadrotor with disturbance observer and position estimator. *Robotics and Autonomous Systems*, 79, 87-98.

[10] Huo, X., Huo, M., & Karimi, H. R. (2014). Attitude stabilization control of a quadrotor UAV by using backstepping approach. *Mathematical Problems in Engineering*, 2014.

[11] Qi, Y., Zhou, S., Kang, Y., & Yan, S. (2016). Formation control for unmanned aerial vehicles with directed and switching topologies. *International Journal of Aerospace Engineering*, 2016.

[12] Qi, Y., Zhou, S., Kang, Y., & Yan, S. (2016). Formation control for unmanned aerial vehicles with directed and switching topologies. *International Journal of Aerospace Engineering*, 2016.

[13] Han, L., Dong, X., Li, Q., & Ren, Z. (2017). Formation tracking control for time-delayed multi-agent systems with second-order dynamics. *Chinese Journal of Aeronautics*, 30(1), 348-357.

[14] Han, L., Dong, X., Li, Q., & Ren, Z. (2017). Formation tracking control for time-delayed multi-agent systems with second-order dynamics. *Chinese Journal of Aeronautics*, 30(1), 348-357.

[15] Abbas, R., & Wu, Q. (2015). Tracking formation control for multiple quadrotors based on fuzzy logic controller and least square oriented by genetic algorithm. *The Open Automation and Control Systems J*, 7, 842-850.

[16] Wang, R., & Liu, J. (2017). Adaptive formation control of quadrotor unmanned aerial vehicles with bounded control thrust. *Chinese Journal of Aeronautics*, 30(2), 807-817.

[17] Zheng, Z., & Song, S. (2014). Autonomous attitude coordinated control for spacecraft formation with input constraint, model uncertainties, and external disturbances. *Chinese Journal of Aeronautics*, 27(3), 602-612.



- [18] Zhang, J., Qinglei, H. U., Danwei, W. A. N. G., & Wenbo, X. I. E. (2017). Robust attitude coordinated control for spacecraft formation with communication delays. *Chinese Journal of Aeronautics*, 30(3), 1071-1085.
- [19] Lee, K. U., Choi, Y. H., & Park, J. B. (2017). Backstepping Based Formation Control of Quadrotors with the State Transformation Technique. *Applied Sciences*, 7(11), 1170.
- [20] Hung Pham, Scott A. Smolka and Scott D. Stoller.(2016). A Survey on Unmanned Aerial Vehicle Collision Avoidance Systems. Department of Computer Science, Stony Brook University, Stony Brook, NY, USA.
- [21] Lao, M., & Tang, J. (2017). Cooperative Multi-UAV Collision Avoidance Based on Distributed Dynamic Optimization and Causal Analysis. *Applied Sciences*, 7(1), 83.
- [22] Zhang, M. (2017). Formation flight and collision avoidance for multiple UAVs based on modified tentacle algorithm in unstructured environments. *PLoS one*, 12(8), e0182006.
- [23] Chee, K. Y., & Zhong, Z. W. (2013). Control, navigation and collision avoidance for an unmanned aerial vehicle. *Sensors and Actuators A: Physical*, 190, 66-76.
- [24] Rambabu, R., Bahiki, M. R., & Ali, S. A. M. (2015). Relative position-based collision avoidance system for swarming uavs using multi-sensor fusion. *ARNP J. Eng. Appl. Sci*, 10(21), 10012-10017.
- [25] Alejo, D., Conde, R., Cobano, J. A., & Ollero, A. (2009, April). Multi-UAV collision avoidance with separation assurance under uncertainties. In *Mechatronics, 2009. ICM 2009. IEEE International Conference on* (pp. 1-6). IEEE.



**Kheireddine CHOUTRI** was born in Constantine, Algeria, on 26 February 1992. He received the Master degree in Aeronautical Engineering from the Aeronautics Institute of Blida, Algeria, in 2015. In this same year, he started his doctoral studies in the field of Aerial Robots in the Aeronautics and spatial studies Institute of SAAD DAHLAB Blida 1 University - Blida, Algeria. His current research activities include UAV Guidance, Navigation and Control, Multi agents system.



**Mohand LAGHA** was born in Tizi-ouzou, Algeria, on 30 June 1976. He received the Engineer Diploma in Aeronautical Engineering from the Aeronautics Institute of Blida, Algeria, in 2000, the M.Sc. in Aeronautics Sciences from the SAAD DAHLAB University of Blida, Algeria, in 2003. He received the Ph.D. degree (with honors) in Aeronautical Engineering at the

Aeronautics Department of SAAD DAHLAB Blida University on 3rd July 2008, and the habilitation (HDR) on September 2010. At present he is Full Professor in Aeronautics and spatial studies Institute of SAAD DAHLAB Blida 1 University - Blida, Algeria. His current research activities include estimation theory, radar signal processing, weather radar signal analysis and UAV applications.



**Laurent DALA** received his PhD in Aerospace Engineering from the University of Manchester. He also graduated from the French Grandes Ecoles in Aerospace Engineering (Ecole Supérieure des Techniques Aérospatiales-ESTA) and in Mechanical and Electrical Engineering (Ecole Spéciale des Travaux Publics, du Bâtiment et de l'Industrie-ESTP). He is a Fellow of the Royal Aeronautical Society, a Chartered Engineer (CEng and Eur-Ing) and the Past

President of the Aeronautical Society of South Africa (AeSSA). Laurent was titular of the Chair in Aerospace Engineering and Head of the Aerospace Research Group at the University of Pretoria (South Africa) till October 2016. He has a very long and successful experience in applied and fundamental research in international aerospace projects, such as in the FP6 European project NACRE (New Aircraft Concepts Research), where he was the Chairman of the Advisory Group. His research is based on a multi- and cross- discipline approach, combining analytical/engineering (using Asymptotic Theory for instance), experimental and computational methods. In 2016, Laurent joined Northumbria University where he is the Head of Mechanical Engineering. His fields of expertise are Aerodynamics, Aeroelasticity, Aeroacoustics, Flight Mechanics and Multidisciplinary Optimisation Methods.